Egypt. J. Chem. **Vol. 65,** No. SI: 13B pp. 1 - 7 (2022)

Egyptian Journal of Chemistry

http://ejchem.journals.ekb.eg/

High efficiency double-channel fluorescent Nickel (II) complex: syntheses, X-ray crystal structures, spectroscopy and surface checking Hirshfeld

[1]Haitham kadhim Dakheel , [2]Haider M. Hessoon

[1]Department of Chemistry, College of Education, University of Al-Qadisiyah , Diwaniya, Iraq
[2]Department of Chemistry, College of Science, University of AL-Qadisiyah, Dewanyiah, Iraq

Abstract

In this paper novel Ni(II) complex, derived from the salemo-based Nickel(II) complex was synthesized and characterized by elementary analysis, infrared spectroscopy, ultraviolet-visible absorption spectroscopy, single-crystal diffraction and Hirshfeld surface analyses. Solution of this complex could be used detect S^{2-} with high sensitivity and selectivity in the presence of different anions via and spectra analysis with the naked eye. The solution colour was converted from colourless to bright yellow by the addition of S2 fibre. UV absorption, fluorescence and other methods of characterization were performed and a action mechanism was developed. I also visually inspected H_2S gas, and the Ni(II) complex was also able to detect S^{2-} in H_2S gas and its possible use in biology and medicine is highlighted.

Keywords: fluorescence , X-ray single crystal , Spectroscopy , Hirshfeld surface analysis,schiff base

1. Introduction

As nickel (II) ions are well known and sulfur ions play important roles in life, sulfur is common in nature and has some toxicity [1-6] .The discharge of sulfur-containing pollutants severely threatens the atmosphere and human health [7.8]. This not only pollutes the soil and water supply, but also releases acid hydrogen sulfide gas for air pollution due to the presence of sulfur ion [8-11]. In addition to many detection methods, fluorescence detection has the advantages of easy operation, large sensitivity and strong selectivity and is commonly used in optical imaging ion detection [12-14]. Sensitive detection of hydrogen content of sulfide in living cells will help to study the effect of hydrogen sulfide on biological properties [15-18]. The complexities of his members were prepared in our research this sulfur ion detection and he possessed selective and sensitive high [19-24].

Experiment

Materials and measurements

Chemicals obtained from Alpha and used without additional purification. Analytical reagents. The accurate analysis of the elements was measured as well as the study of atomic emission spectrometry. The nuclear magnetic resonance spectrometry was recorded. The meltdown point of the infrared spectrum was determined as well as the UV spectrum absorption.

Preparation of Ligand

Chart 1 shows how to prepare lycand. Lycand under study was manufactured ethane 1,2-bis (aminoxy) following published methods [27-29]. Slowly Licand was prepared by adding 1.2 bis (aminoxy) ethan (3.0 mmol, 271.9 mg) dissolved in absolute ethanol (20 ml) on 2-hydroxy-3-methoxybenzaldehyde solution (3.0 mmol or 455.99 mg). The combination was moved in the magnetic motor for 5-6 hours, the solution was concentrated in the vacuum and the column chromatography was used for the separation of 6-methoxy2- [S-(1-ethyloxyamide)] oxyme-1-phenol (L). Ethanol solution (L) (2.0 mmol 448.06 mg) directly interacted with 2-hydroxy-5-methyl benzaldehyde

the 6-methoxy-2-[O-(1-ethyloxyamide)]oxime-1-phenol (LH). The (LH) ethanol solution (2.0 mmol 448.06 mg) was directly reacted with 2-hydroxy-5-

*Corresponding author e-mail: Haitham.kadhim@qu.edu.iq (Dr.Haitham kadhim Dakheel).
Receive Date: 31 December 2020, Revise Date: 07 October 2021, Accept Date: 19 June 2022
DOI: 10.21608/EJCHEM.2022.56091.3203

methylbenzaldehyde (2.0 mmol, 344.16 mg) by one-pot form for obtaining H_2L.yield is 49.8% ;M.p.' 111–116 C; Calcd Anal. for $C_{21}H_{20}N_2O_5$: C, 62.78; H, 5.85; N, 8.13; Found: C, 62.19; H, 5.79; N, 8.09; . 1H-NMR (500 MHz, $CDCl_3$): d 10.79 (s , 1H) , 9.79 (s , 1H), 9.21 (s , 1H), 8.32 (s , 1H), 7.89 (d,J ¼ 8.4 Hz , 1H), 7.77 (s , 2H), 7.49 (s , 1H), 7.35 (t, J ¼ 7.2 Hz , 1H), 7.19 (d, J ¼ 9.1 Hz , 1H), 6.89 (dd, J ¼ 7.5 ,1.8 Hz , 1H), 6.86 (dd, J ¼ 13.8, 11.0 Hz , 2H), 4.49 (s , 4H), 3.89 (s , 3H).

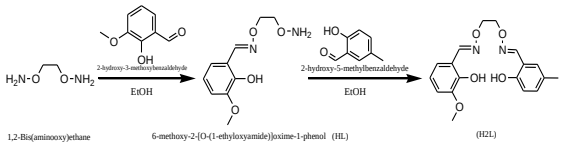

Scheme 1 Synthetic path to H_2L.

Synthesis method of the Ni(II) complex

Solution (3 ml) of nickel 2.6 H_2L (7.41 mg, 0.02 mmol). After mixing it immediately became a transparent brown solution and it was moved for 5 minutes at room temperature. To remove impurities, the solution was filtered, a bottle for one week to evaporate. [30-33] One crystal was obtained in the form of a block structure that was suitable for X-ray diffraction analysis.Rate of return: yield is 40.52%. ;M.p. 167–169 C˚; Calcd Anal. for [Ni (H2L)]; [C18H18N2NiO5): (C, 53.91; H, 4.52; N, 6.99; Ni, 14.64) Funded (C, 54.11; H, 4.32; N, 6.77; Ni, 14.54).

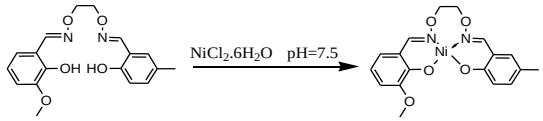

Scheme 2 Synthetic path to Ni(II)- complex.

Results and Discussion

Spectroscopy of UV-vis absorption

For the purpose of measuring the absorption of the UV spectrum 2 ml of the nickel complex was added in the sample cell to test the UV absorption spectrum as a control experiment and then added 0.9 ml ethanol and 0.1 ml deionized water gave wavelength at 401 nm due to the absorption of complex nickel for electron-d transport. (1 ml) of a complex nickel solution The wavelength and absorption were measured and did not give any change in the UV spectrum referring to its stable complex nickel prepared [33,34]. The UV absorption spectrum of UV light was found to have changed dramatically only when sulphur ion was added and there were new peaks at 352 and 419 nm. A control experiment was conducted with ultraviolet absorption peaks of ethanol/water (10:1) indicating a nickel complex [35-37]. As in figure 1, the color of the solution varied considerably between colorless and light yellow. After the addition of other anions, the solution did not change the color and absorption force of UV radiation significantly but only changed after the increase of the individual addition to the sulfur ion. The sample molecules had good sensitivity and selectivity to recognize the sulfur ion and the result was unchanged by other typical ions (shape. 2). The peak absorption breadth was obtained at 419 nm when the negative sulfur ion was added. 3). This graph clearly shows that the rise in the number of other anions does not indicate any consistency between lycand and ions being experimented with. Therefore the complex nickel prepared can easily and effectively detect negative sulfur ion. In the UV calibration experiment, when adding 2 ml of sulfur ion solution new absorption peaks appeared at 352 and 419 nm with increased sulfur ion concentration as shown in the figure. 4.

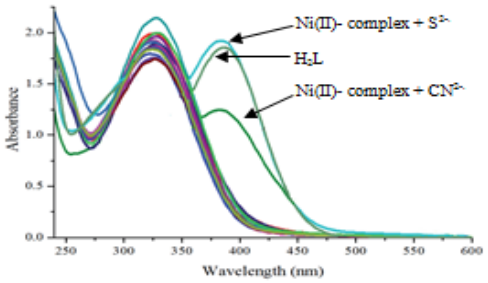

Fig. 1 Spectral absorption of the solution Ni(II) complex ($5x10^{-5}$M) in the absence and presence of different anions (Cl^-, ClO_4^-, CN^- , CO_3^{2-} , $H_2PO_4^-$, HCO_3^-,HPO_4^-, HS^-, I^-, NO_2^-, NO_3^-, CH_3COO^-, and S^{2-}

Spectroscopy of fluorescence

When 1 equal to the ethanol solution was added to the probe molecules with a concentration of 10 times the sixteen anions of ethanol/water (10:1), a bright yellow color change was observed with the naked eye due to the activity of the probe molecule and the negative sulfur ion. Besides, when the excitation wavelength was 378 nm, the number of fluorescent emissions was small, but at sulphur additives there was a high emission of 458 nm and a red displacement of 28 nm, as in the figure. 5). The sensor molecule has been shown to be able to detect sulfur ion through two channels. Furthermore, the control experiment tested the peak lycand emission in ethanol/water solution (10: 1) It was found when adding sulfur ion - a nickel complex in ethanol where its top gave an emission as

shown in figure 6 that adding other anions to the solution does not have a significant impact on the capability of determining negative sulfur ion [38.30]. The result was that the molecule examined had a strong anti-interference effect in the spectrum of brilliance to sulfur ion. An experiment was conducted to verify the correlation ratio between the probe molecule and the sulphur ion. In the calibration experiment, the wavelength of the excitement was 375 nm as in figure 7 as the ethanol solution of the probe, a drop was added on different quantities of sulfur ion, the fluorescent strength of the main peak was greatly increased with a steady red drift. The glitter did not increase when the sulfur ion was applied to the equivalent of 1.0 indicates the calibrated fluorescent finish [40].

Binding constant for complex nickel and sulfur ion receptor molecules was k 0.6 x 104 compared to LCD 3.34 x 10-8. Furthermore, pH control experiments showed that the nickel ion sensor complex would effectively classify sulfur ion in the pH 4-9 range (shape. 9).

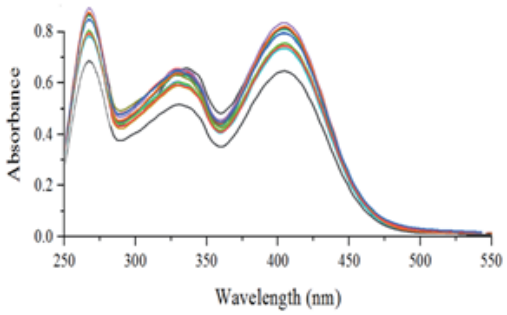

Fig. 2 In the presence of sulfur ions, were added ina variety of anions (Cl^- , ClO_4^-, CN^- , CO_3^{2-} , $H_2PO_4^-$, HCO_3^-,HPO_4^-, HS^-, I^-, NO_2^-, NO_3^-, CH_3COO^-, and S^{2-}) the peak at 401 nm did not change at all.

Table 1 Interventions of the presumed hydrogen (Å,°) association of nickel complex

D–X···A	C1–H1A···O2	C3–H3···O3	C6–H6···O3	C10–H10B···O5	C11–H11B···O5
d(D–X)	0.93	0.92	0.94	0.95	0.95
d(X···A)	2.34	2.52	2.14	2.35	2.36
d(D···A)	3.123(10)	3.232(8)	3.216(10)	3.232(10)	3.454(10)
∠D–X···A	115	138	139	133	159
Symmetry code	−x,1−y,1−z	−x,1−y,2−z	−x,1−y,2−z	−1 + x,1 + y,−1 + z	x,1 + y,−1 + z

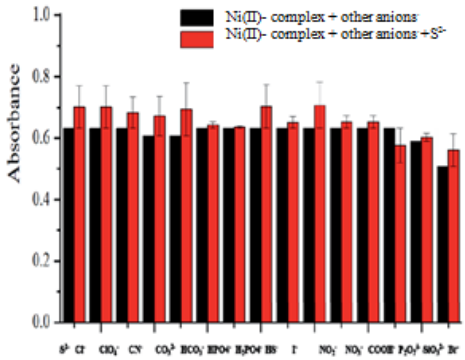

Fig. 3 The black strip illustrates the Ni(II) complex solution absorption intensity at 419 nm when the S^{2-} was added and the red strip demonstrates the Ni(II) complex solution with an absorbance intensity of 419 nm when different anions and S^{2-} have been added.

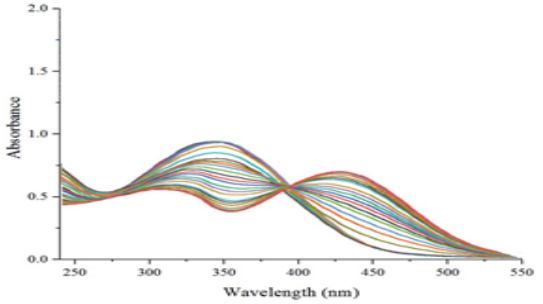

Fig. 4 Shifts in the spectrum of the Ni(II) complex solution sample (5 = 10 alternatives to 5 m) with the increase of S^{2-} (0–1.0 equivalents). the bright yellow change of the probe Ni(II) complex solution is detected by the naked eye before and after adding S^{2-} (1 equivalent).

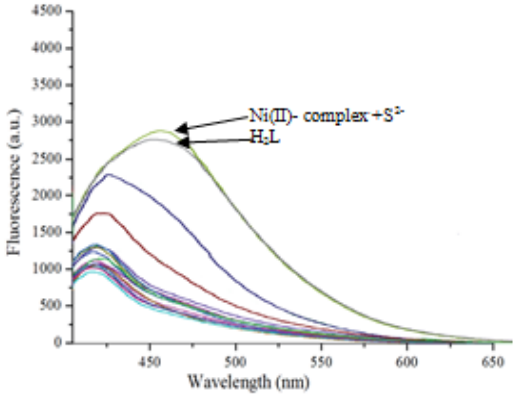

Fig. 5 1 mL of Ni(II) complex solution (5 x 10^{5-} M) was taken in the sample cell and 1 mL of different anion solutions (Cl^-, ClO_4^-, CN^- , CO_3^{2-} , $H_2PO_4^-$, HCO_3^-,HPO_4^-, HS^-, I^-, NO_2^-, NO_3^-, CH_3COO^-, and S^{2-}) were added to test the change in the fluorescence spectrum.

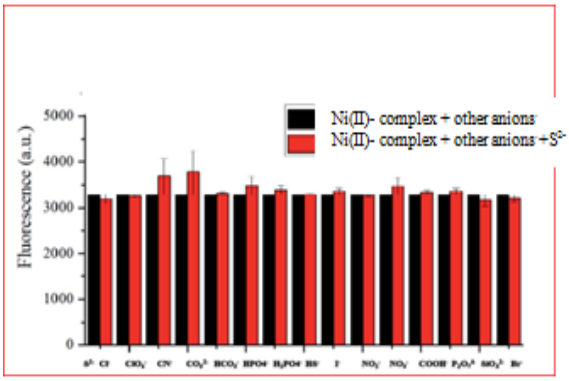

Fig.6 500 µL various anions (Cl^-, ClO_4^-, CN^-, CO_3^{2-}, $H_2PO_4^-$, HCO_3^-,HPO_4^-, HS^-, I^-, NO_2^-, NO_3^-, CH_3COO^-, and S^{2-})have been added to a 1 mL solution Ni(II) complex and 500 µL of S^{2-} has been added to test for an effect on the fluorescence of the system.

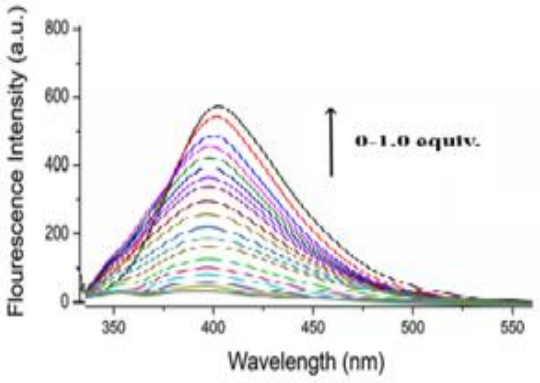

Fig. 7 Ni(II) complex solution (5 x 10^{5-} M) fluorescence spectrum when increased by S^{2-} (0-1.0 equivalent).

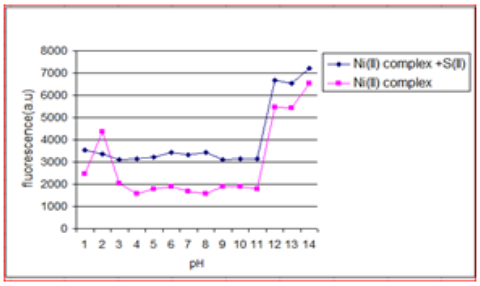

Fig. 8 The black. dotted line. diagram shows. the Ni(II) complex fluorescence. spectrum at. different pH. conditions; the. red dotted line. shows the. fluorescence spectrum. test results. with the. addition of. S^{2-}

Mechanism research

The peak absorption of its molecule is 401 nm resulting from the association of negative sulfur ion, positive nickel ion and absorption peaks of 352 and 419 nm. With the high concentration of sulfur ion, the peak decreased at 352nm, and the peak absorption rose at 419nm. The ratio signal in the linear range changed by a factor of 20. This sample has no response to different anions other than sulfur ion and cyanide and has good selectivity. The solution changed from colorless to light yellow before and after the reaction, so, the sulfur ion can measure colors with a high sensitivity [41,42]. She served as a donor to the Nickel Glistening Experiment as a future for the formation of a nickel complex ,Due to the cooling effect of Ni^{2+}, the brilliance disappeared.

The excess S^{2-} plus has also been added and shine restored, demonstrating stronger binding capabilities than the S^{2-} and Ni^{2+}, restoring the Ligandi brilliance.The mass spectrometry showing that a substantial peak at m / z^+ 344.14 was compatible with the ligand molecular ion peak Fig. 9, and a peak at m / z^+ 401.04 Fig. 10 was due to Ni (II) complex. Then added NaS and conducted additional mass spectrometry,a molecular ion peak that corresponded to the ligand appeared at m / z^+ 344.14 . S^{2-} combines. With nickel ion to form nickel sulfide in the complex is quite clear simultaneously nickel ion obtained by the complex nickel returned to lycand as shown in chart 3.

Gas detection H_2S

Sodium sulfide has been added sulfuric acid (60 ml, 3 m1 -) preparing the steam hydrogen sulfide, which has been injected sequentially into pure ethanol on nickel ion [43.44]. With hydrogen sulfide the color of the solution deepened to a pale yellow color and was easily identified by the naked eye. However, the pure ethanol solution did not significantly change shape 10. Color shift duration from one to three minutes seen in ethanol solution and nickel complex solution when introducing hydrogen sulfide gas [45-47]. The color remained essentially unchanged for 5 hours, indicating that the probe has a strong stability in the identification of hydrogen captide and can meet the needs of analysis and detection. By adding hydrogen captide gas and water shortage to the solution, preventing the formationof the intracellular hydrogen bond, the development of acidic environments has broken the static environment of molecules and turned the solution brown. The color of the solution changed from yellow to brown. When water was applied to a complex nickel solution containing hydrogen sulfide

gas.

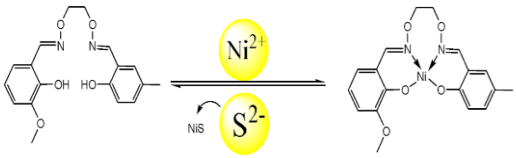

Scheme 3 Schematic diagram for configuring the sample molecule and visualizing two-channels of S^{2-}

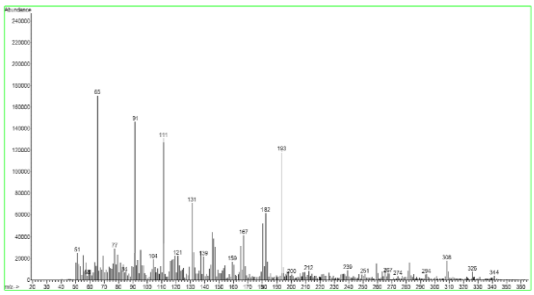

Fig. 9 Mass spectrum of salemo-based ligand H_2L

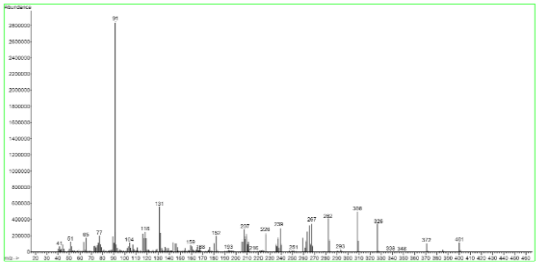

Fig. 10 Mass spectrum of Nickel(II) complex

Analysis of Hirshfeld surfaces

Surface analysis from Hirshfeld can be used to analyze weak crystal interactions and species can also be visually displayed. Of interactions. Between molecules. In different. Areas through colors [48-50]. The superficial analysis of the Hirschfeld complex is presented Figure 11 shows the difference in surface structure of Hirschfeld suggests that the intermolecular complexes [51,52]. For the complex red and blue surfaces are compatible with supplementary areas. The interaction between C–H---O can be attributed to the red surface and the blue surface can be attributed to C---H,H---H and C---C contacts. As regards the white surface, it does not have hydrogen bonds due to the long distancebetween the molecule[53,54]s. The 2D fingerprint produced can be used for quantitative studies of the interactions between hydrogen molecules. Figure 10 shows the fingerprints of the complex .Blue regions show different interaction between molecules, The interaction of C-H / H – C, O – H / H – O and H – H / H – H was 18.9%, 7.9%, and 53.7% of the total complex surfaces[55].The hydrogen communication reactions of the compound are greatly increased which correspond to the description of crystal structures.

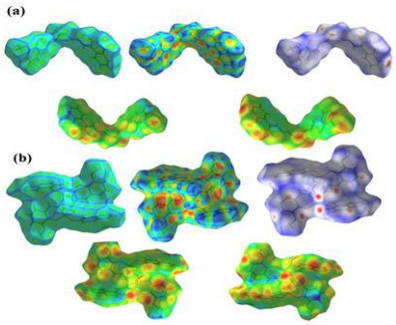

Figure 11. Hirshfeld surface. analyses mapped. with curvedness., shape-index., d_{norm}, d_e., and. d_i of H_2L. and its. Ni(II) complex.

The crystal structure of Ni-complex

As shown in figure 12, the nickel complex has a symmetrical single-core structure [56-59]. In the crystal structure of the nickel node it turns out to be quadruple harmony with the nickel atom. There is only one pair of hydrogen bonds within the molecules in the crystal structure of the node[60-64]

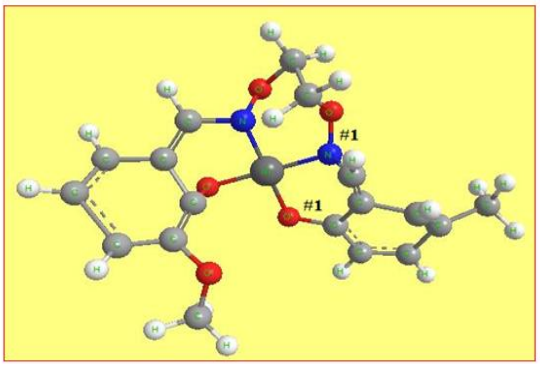

Fig. 12. Molecule. structure and. atom numberings. of the complex. (hydrogen. atoms are. omitted for. clarity). atom. of the complex

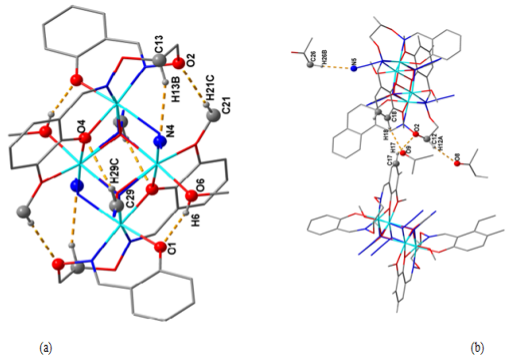

Figure 13 (a) Intramolecular hydrogen bond interactions of complex, (b) intermolecular hydrogen bond interactions of complex interactions,

Conclusion

We prepared this study of a nickel complex for the purpose of diagnosing sulfur by the spectrum of UV absorption and shine. Spectrometry showed sulfur ion

when added to the nickel complex where it is a stable shape as shown. in figure 1. After the addition of sulfur ion, the peak absorption disappeared at 401 nm and new absorption peaks appeared at 352 and 419 nm, in the study of glamor, the reaction system produced a new peak of 458 nm with intensity and longer wavelength when sulfur ion was added to the nickel complex. The intensity of shine is shown at 458 nm in figure 6. Thereafter, more nickel complexity was added to sulfur and the strength of glamor was not significantly affected. This shows that the nickel complexity of this research has a strong selectivity to detect sulfur ions. My experimental results showed that the nickel complex has the potential to detect sulfur ion in gas.

References

[1] A. Tzubery, N. Melamed-Book, E. Y. Tshuva, Dalton Trans. 2018, 47, 3669.
[2] L. W. Zhang, Y. Zhang, Y. F. Cui, M. Yu, W. K. Dong, Inorg. Chim. Acta 2020, 506, 119534.
[3] S. Z. Zhang, J. Chang, H. J. Zhang, Y. X. Sun, Y. Wu, Y. B. Wang, Chin. J. Inorg. Chem. 2020, 36, 503.
[4] H. R. Mu, X. X. An, C. Liu, Y. Zhang, W. K. Dong, J. Struct. Chem. 2020, 61, 1155.
[5] M. Shebl, O. M. I. Adly, E. M. Abdelrhman, B. A. El-Shetary, J. Mol. Struct. 2017, 1145, 329.
[6] M. Shebl, J. Coord. Chem. 2009, 62, 3217.
[7] S. Akine, W. K. Dong, T. Nabeshima, Inorg. Chem. 2006, 45, 4677.
[8] Z. L. Wei, L. Wang, S. Z. Guo, Y. Zhang, W. K. Dong, RSC Adv. 2019, 9, 41298.
[9] M. B. Solomon, A. Rawal, J. M. Hook, S. M. Cohen, C. P. Kubiak, K. A. Jolliffe, D. M. D'Alessandro, RSC Adv. 2018, 8, 24128.
[10] D. Park, C. I. Jette, J. Kim, W. O. Jung, Y. Lee, J. Park, S. Kang, M. S. Han, B. M. Stoltz, S. Hong, Angew. Chem., Int. Ed. 2020, 59, 775.
[11] Y. Yao, H. Y. Yin, Y. Ning, J. Wang, Y. S. Meng, X. Huang, W. Zhang, L. Kang, J. L. Zhang, Inorg. Chem. 2019, 58, 1806.
[12] S. Mirza, H. Chen, S. M. Chen, Z. G. Gu, J. Zhang, Cryst. Growth Des. 2018, 18, 7150.
[13] S. W. Kwak, H. Jin, J. H. Lee, H. Hwang, M. Kim, Y. Kim, Y. Chung, K. M. Lee, M. H. Park, Inorg. Chem. 2019, 58, 2454.
[14] S. Akine, M. Miyashita, S. Piao, T. Nabeshima, Inorg. Chem. Front. 2014, 1, 53.
[15] X. X. An, Q. Zhao, H. R. Mu, W. K. Dong, Crystals 2019, 9, 101.
[16] R. Yerrasani, M. Karunakar, R. Dubey, A. K. Singh, T. R. Rao,J. Mol. Liq. 2017, 248, 214.
[17] L. Xu, M. Yu, L. H. Li, J. C. Ma, W. K. Dong, J. Struct. Chem. 2019, 60, 1358.
[18] D. Yuan, N. Cai, J. Xu, D. Miao, S. Zhang, S. E. Woodfine, D. Plana, C. S. Hawes, M. Watkinson, ChemPlusChem 2020, 85, 1210.
[19] M. Yu, Y. Zhang, Y. Q. Pan, L. Wang, Inorg. Chim. Acta 2020, 509, 119701.
[20] Y. X. Sun, Y. Q. Pan, X. Xu, Y. Zhang, Crystals 2019, 9, 607.
[21] Y. Zhang, L. Z. Liu, Y. D. Peng, N. Li, W. K. Dong, Transition Met. Chem. 2019, 44, 627.
[22] Q. P. Kang, X. Y. Li, Z. L. Wei, Y. Zhang, W. K. Dong, Polyhedron 2019, 165, 38.
[23] X. X. An, Z. Z. Chen, H. R. Mu, L. Zhao, Inorg. Chim. Acta2020, 511, 119823.
[24] Y. Q. Pan, Y. Zhang, M. Yu, Y. Zhang, L. Wang, Appl. Organomet. Chem. 2020, 34, e5441.
[25] C. Liu, X. X. An, Y. F. Cui, K. F. Xie, W. K. Dong, Appl. Organomet. Chem. 2020, 34, e5272.
[26] A. Taha, A. A. M. Farag, O. M. I. Adly, N. Roushdy, M. Shebl, H. M. Ahmed, J. Mol. Struct. 2017, 1142, 66.
[27] C. Liu, Z. L. Wei, H. R. Mu, W. K. Dong, Y. J. Ding, J. Photochem. Photobio. A 2020, 397, 112569.
[28] L. Wang, Z. L. Wei, C. Liu, W. K. Dong, J. X. Ru, Spectrochim. Acta a 2020, 239, 118496.
[29] X. Y. Li, Q. P. Kang, C. Liu, Y. Zhang, W. K. Dong, New J. Chem. 2019, 43, 4605.
[30] Q. Zhao, X. X. An, L. Z. Liu, W. K. Dong, Inorg. Chim. Acta2019, 490, 6.
[31] Y. Zhang, Y. Q. Pan, M. Yu, X. Xu, W. K. Dong, Appl. Organomet. Chem. 2019, 33, e5240.
[32] L. Z. Liu, M. Yu, X. Y. Li, Q. P. Kang, W. K. Dong, Chin. J. Inorg. Chem. 2019, 35, 1283.
[33] J. Chang, S. Z. Zhang, Y. Wu, H. J. Zhang, Y. X. Sun, Transition Met. Chem. 2020, 45, 279.
[34] Y. Zhang, M. Yu, Y. Q. Pan, Y. Zhang, L. Xu, X. Y. Dong, Appl. Organomet. Chem. 2020, 34, e5442.
[35] Z. L. Wei, L. Wang, J. F. Wang, W. T. Guo, Y. Zhang, W. K. Dong, Spectrochim. Acta a 2020, 228, 117775.
[36] M. Shebl, J. Coord. Chem. 2016, 69, 199.
[37] L. Wang, Z. L. Wei, Z. Z. Chen, C. Liu, W. K. Dong, Y. J. Ding, Microchem. J. 2020, 155, 104801.
[38] L. Wang, Y. Q. Pan, J. F. Wang, Y. Zhang, Y. J. Ding, J. Photochem. Photobio. A 2020, 400, 112719.
[39] Y. Q. Pan, X. Xu, Y. Zhang, Y. Zhang, W. K. Dong, Spectrochim. Acta a 2020, 229, 117927.
[40] Q. P. Kang, X. Y. Li, L. Wang, Y. Zhang, W. K. Dong, Appl. Organomet. Chem. 2019, 33, e5013.
[41] L. Z. Liu, L. Wang, M. Yu, Q. Zhao, Y. Zhang, Y. X. Sun, W. K. Dong, Spectrochim. Acta a 2019, 222, 117209.
[42] M. Yu, H. R. Mu, L. Z. Liu, N. Li, Y. Bai, X. Y. Dong, Chin. J. Inorg. Chem. 2019, 35, 1109.
[43] X. X. An, C. Liu, Z. Z. Chen, K. F. Xie, W. K. Dong, Crystals2019, 9, 602.

[44] L. Wang, Z. L. Wei, M. Yu, Y. Q. Pan, Y. Zhang, W. K. Dong, Chin. J. Inorg. Chem. 2019, 35, 1791.
[45] Y. F. Cui, Y. Zhang, K. F. Xie, W. K. Dong, Crystals 2019, 9, 596.
[46] M. Shebl, M. Saif, A. I. Nabeel, R. Shokry, J. Mol. Struct. 2016, 1118, 335.
[47] H. R. Mu, M. Yu, L. Wang, Y. Zhang, Y. J. Ding, Phosphorus, Sulfur Silicon Relat. Elem. 2020, 195, 730.
[48] R. N. Bian, J. F. Wang, Y. J. Li, Y. Zhang, W. K. Dong, J. Photochem. Photobiol. A. 2020, 400, 112719.
[49] X. Xu, R. N. Bian, S. Z. Guo, W. K. Dong, Y. J. Ding, Inorg. Chim. Acta 2020, 513, 119945.
[50] A. Li, E. Rentschler, Polyhedron 2018, 154, 364.
[51] M. Shebl, J. Mol. Struct. 2017, 1128, 79.
[52] H. S. Seleem, B. A. El-Shetary, S. M. E. Khalil, M. Mostafa, M. Shebl, J. Coord. Chem. 2005, 58, 479.
[53] M. Shebl, Spectrochim. Acta a 2009, 73, 313.
[54] G. Ambrosi, M. Formica, V. Fusi, L. Giorgi, M. Micheloni, Coord. Chem. Rev. 2008, 252, 1121.
[55] M. Shebl, Spectrochim. Acta a 2008, 70, 850.
[56] H. F. El-Shafiy, M. Shebl, J. Mol. Struct. 2019, 1194, 187.
[57] M. Shebl, Spectrochim. Acta a 2014, 117, 127.
[58] M. Shebl, M. A. El-ghamry, S. M. E. Khalil, M. A. A. Kishk, Spectrochim. Acta a 2014, 126, 232.
[59] M. Shebl, S. M. E. Khalil, A. Taha, M. A. N. Mahdi, Spectrochim. Acta a 2013, 113, 356.
[60] H. S. Seleem, B. A. El-Shetary, M. Shebl, Heteroatom. Chem. 2007, 18, 100.
[61] M. Shebl, H. S. Seleem, B. A. El-Shetary, Spectrochim. Acta a2010, 75, 428.
[62] M. Shebl, S. M. E. Khalil, A. Taha, M. A. N. Mahdi, J. Mol. Struct. 2012, 1027, 140.
[63] M. Shebl, S. M. E. Khalil, S. A. Ahmed, H. A. A. Medien, J. Mol. Struct. 2010, 980, 39.
[64] B. Gao, D. Zhang, Y. Li, Opt. Mater. 2018, 77, 77